NIGERIAN JOURNAL OF MATERIALS SCIENCE AND ENGINEERING
NJMSE
ISSN 214-453-2

ELECTROCHEMICAL AND STRUCTURAL CHARACTERIZATION OF NICKEL OXIDE FILLED ACTIVATED CARBON FOR SUPERCAPACITOR ELECTRODE APPLICATION

T. O. AHMED*, O. O. OGUNLEYE, I. A. GALADIMA[1], B. A. SULLE[1] AND A. BELLO[2]
Department of Physics, Federal University Lokoja, Kogi State, Nigeria
[1]Department of Physics, Ahmadu Bello University, Zaria, Nigeria
[2]Department of Physics, Faculty of Natural & Agricultural Sciences, University of Pretoria, South Africa
[tajudeen.ahmed@fulokoja.edu.ng]

ABSTRACT
We have demonstrated that activated carbon could be produced via microwave-assisted activation at a much shorter time (ranging from 2-5 min) and reduced cost compared to the conventional activation method embraced by most researchers in the production of activated carbon. The research work is not only limited to surface chemistry and adsorption studies but also includes structural, microstructural and electrochemical studies/investigations of the produced Nickel Oxide Filled Activated Carbon (NOFAC). Its uniqueness is tied to cost effectiveness and the use of agricultural waste product. Activated carbon filled with nickel oxide was prepared via microwave-assisted chemical activation using coconut shell, palm kernel shell and their mixture with potassium hydroxide as activating agent. The effect of the incorporation of NiO on the structure and surface chemistry of the raw materials after activation was studied employing Fourier Transform Infra-Red (FTIR) Spectroscopy, Transmission Electron Microscopy (TEM) and X-ray Diffraction (XRD) analysis. The electrochemical characteristics were investigated employing Cyclic Voltammetry (CV), Galvanostatic Charge-Discharge (GCD) analysis and Electrochemical Impedance Spectroscopy (EIS). The FTIR spectroscopy confirmed the existence of strong interfacial interaction between NiO and the host matrices showing creation and annihilation of absorption bands in the IR spectra with significant absorptions observed below 500cm^{-1} for nickel oxide. The TEM results showed that the microstructural evolution of host matrices is as a result of incorporation of NiO and activation using microwave power respectively. A follow-up with XRD confirmed the presence of anomalous graphite structure surrounded by traces of impurities resulting from the activating agent. Finally, the scan rate studies revealed activated palm kernel shell as the best candidate with better current response, higher value of specific capacitance and better electrochemical behaviour.

Keywords: *Activated carbon, nickel oxide, microwave activation, supercapacitor electrode, microstructures, electrochemical behaviour.*

1.0 Introduction

Energy has been a prime focus over the years for many societies. This challenge has however caused a revolution of ideal energy storage devices. An ideal energy storage device is characterized with high power density and high energy density. Among all other energy storage devices, electrochemical supercapacitors (ES) have matured significantly over the last decade and emerged with the potential to facilitate major advances in energy storage devices. They exhibit higher power density than batteries and solar cells and higher energy density than conventional capacitors because of their unique charge storage mechanisms (Halper *et al.* 2006).

Electrochemical supercapacitors are emerging as devices of prime importance owing to their infinite energy lifespan. Traditional power sources and batteries, essential to our personal electronic devices and automobiles, don't store that much energy. Due to their high storage energy capacity, supercapacitors are finding increased usage in portable electronic devices like MP3 players, mobile phones and palm pilots. Other benefits, like short charging times and high performance in low temperatures, could lead to new applications such as power electronics, large scale transport systems comprising subway trains and buses, energy storage at intermittent generators including windmills, and smart grid applications (Jampani *et al.* 2010, Halper *et al.* 2006).

Commercially available activated carbons (ACs) are usually used for the fabrication of electrode materials for electrochemical supercapacitors and these are usually produced from coconut shell, coal and peat (Yang *et al.* 2010, Ge *et al.* 2015, Acavedo *et al.* 2015 and Salame *et al.* 2001). In recent times, the quest for production of efficient, low-cost, scalable, locally available and renewable carbon materials for absorbent and energy storage applications has shifted the attention of most researchers to the use of biomass or organic waste materials (Park *et al.* 2006). However, the most embraced methods of activation have been the conventional ones for the production of activated carbons for absorbent applications and environmental remediation (Ofomaja *et al.* 2011, Nunell *et al.* 2015 and Momcilovic *et al.* 2011). In addition to this, there are few or no reports on the use of activated carbon from coconut shell, palm kernel shell and their mixtures for supercapacitor electrode application in Nigeria. Nevertheless most reports are from Europe, Asia and South Africa on the use of activated carbons derived from coconut shell and pine cone and others like

expanded graphite, carbon nanotubes, grapheme, conducting polymer etc. for supercapacitor electrode application (Taberna *et al.* 2003, Roberts *et al.* 2009, Demarconnay *et al.* 2011, Zhang *et al.* 2013 and Bello *et al.* 2014).

Several supercapacitors system based on AC, carbon nanotubes and grapheme have been developed to attain high performance energy storage devices namely; AC//Ni(OH)2 (Wu *et al.* 2008), grapheme//$Ni(OH)_2$ (Wang *et al.* 2010), carbon nanotubes//MnO2 (Aravanda *et al.* 2013), AC//MoO3 (Tang *et al.* 2011). These electrochemical supercapacitor exhibited high energy storage capabilities but these are still far from commercialization due to the poor capacitive performance of the positive electrode materials at high current loading and the corresponding carbon negative materials in a low current utilization (Wang *et al.* 2014). In this study coconut shell, palm kernel shell and their mixture have selected for the development of supercapacitor electrode. Our choice is due to the fact that coconut and palm trees are naturally abundant in Nigeria and Africa and can be easily activated by a facile microwave-assisted activation method that gives better AC and yield and saves time and cost (Mohammadyani *et al.* 2012, Baghbanzadeh *et al.* 2011 and Kappe 2008).

For this research, the coconut and the palm kernel shells used were obtained from the open market where most of them had been dumped as waste products. In our laboratory Nickel Oxide Filled Activated Carbon was produced via microwave-assisted activation at a much shorter time (ranging from 2-5 min.) and reduced cost compared to the conventional activation method embraced by most researchers in the production of activated carbon. This research effort is not only limited to surface chemistry and adsorption studies but also includes structural, microstructural and electrochemical investigations of the produced Nickel Oxide Filled Activated Carbon (NOFAC). Its uniqueness is tied to cost effectiveness and the use of agricultural waste product. The effect of the incorporation of NiO on the structure and surface chemistry of the raw materials after activation was studied employing Fourier Transform Infra-Red (FTIR) Spectroscopy, Transmission Electron Microscopy (TEM) and X-ray Diffraction (XRD) analysis. The electrochemical characteristics were investigated employing cyclic voltammetry, current response, impedance and specific capacitance measurements.

2.0 Materials and Methods

The coconut and palm kernel shells were obtained easily from an open market (Sabon Gari market, Zaria, Kaduna State, Nigeria) where they were being dumped as a waste product. Crushing and sieving of the raw materials were carried out to obtain a fine particle size powder. The raw materials which were powdered samples of coconut shell (CS), palm kernel shell (PS) and a mixture of coconut shell and palm kernel shell (CS+PS) were impregnated with a solution of KOH carbonized for 4 minutes using microwave power. Nickel oxide was then prepared from 1M solution containing $Nicl_2$ and Glycine in the presence of 3M KOH bath using microwave-assisted coprecipitation technique [Kappe 2008, Baghbanzadeh *et al.* 2011 and Mohammadyani *et al.* 2012). The precipitated gel was washed thoroughly with NH_4OH and subsequently heated for 2 minutes using microwave power to pure sample of NiO powder. In order to prepare the metal oxide filled activated carbon, carbonized samples of CS, PS and CS + PS were mixed with NiO powder in the ratio 9:1 by weight respectively for each of the samples and subsequently impregnated with 3M KOH solution.

Each of the dissolved samples was carbonized for another 4 min using microwave power. After carbonization, the activated carbon samples were washed thoroughly with mixture of distilled water and ammonia solution to eliminate the residual activating agent that must have penetrated into the pore spaces and occupied substantial volume of the activated carbon samples. This was done to create large numbers of pore spaces. Subsequently, the activated carbon samples were ground to fine particle sizes and re-heated for a minute to further activate the carbon samples. Finally, the metal oxide filled activated carbon samples were ground again to fine particle sizes.

The bulk density of the nickel oxide filled activated carbon samples was measured using Micrometrics AccuPyc II 1340 (version 1.03). The surface chemistry of the raw materials and the effect of the incorporation of NiO on the surface chemistry of the raw materials after activation were studied using SHIMADZU FTIR-8400S Spectrophotometer at National Research Institute for Chemical Technology (NARICT) Zaria, Nigeria, in transmission mode without KBr. The FTIR spectra were recorded in the 400 to 4600 cm^{-1} frequency range, after 25 scans, with resolution of 2 cm^{-1}. The positions and intensities of the IR bands were processed with Spectral Analysis Software.

Furthermore, the effect of NiO incorporation on the structure and microstructure of the activated carbon was investigated using X-Ray Diffraction Analysis (XRD) and Scanning Electron Microscopy (SEM) respectively. The X-Ray Diffraction (XRD) patterns of the activated carbon samples were collected on an XPERT-PRO Diffractometer (PANalytical BV, Netherlands) operating on a cobalt tube at 35kV and 50mA. The goniometer is equipped with automatic divergence slit and a PW3064 spinner stage. The XRD patterns of the activated carbon samples were recorded in the 10^o – 80^o 2θ range with a step size of 0.017^o and a counting time of 15.24 seconds per step. Qualitative phase analysis of sample was conducted using the X'pert Highscore Plus search match software. As a follow-up to the XRD analysis, the surface morphology of the solid NOFAC samples was investigated using a Zeiss Ultra Plus 55 field emission scanning electron microscope (FE-SEM) operated at 20kV employing secondary electrons signals. The particle size distribution was obtained using Image-J imaging software.

All electrochemical measurements; such as Cyclic Voltammetry (CV), Galvanostatic Charge-Discharge (GCD) and electrochemical impedance spectroscopy

(EIS), were carried out using a Bio-logic SP-300 potentiostat. The three electrode method was employed; where the Activated Carbon (AC) serves as the working electrode, Glassy Carbon Plate (GCP) as the counter electrode and Ag/AgCl (3M KCl) serves as reference electrode in 6M KOH electrolyte, for electrochemical characterization. The AC electrode was prepared using Polyvinylidene Flouride (PVDF) as a binder and N-methylpyrolidine (NMP) solution as dispersant for the three samples (CS, PS and CS+PS). The active material (AC) and Polyvinylidene Flouride (PVDF) were mixed in ratio 9:1 by weight respectively, homogenized and dispersed in N-methylpyrolidine (NMP) solution. The paste was then was then uniformly pasted on a nickel foam current collector and dried at 60^{o}C in an oven for 8 hours to ensure evaporation of the NMP and then allowed to cool down to room temperature.

Cyclic voltammetry (CV) was performed by scanning the potential from - 0.3 to + 0.2 V and the rates were varied from 25 to 100 mVs^{-1}. The charge-discharge analysis was carried out at four different constant currents of 2.5, 5.0, 7.5 and 10.0 mA at potential range of 0 to 0.5 V for the three samples. Finally, the Electrochemical Impedance Spectroscopic (EIS) studies of the three electrode assemblies (CS, PS and CS+PS) were performed in 6M KOH aqueous solution applying a sinusoidal signal of 10 mV peak-to-peak amplitude at a frequency range of 100 mHz to 100 kHz. The impedance data were analyzed in terms of complex impedance using the imaginary and real part plots for the three samples.

3.0 Results and Discussions

The measured bulk density for the mixture of activated coconut and palm kernel shells filled with nickel oxide (CS+PS) was obtained to be (2.185 + 0.0025) g/cm^3 while that for PS and CS are (1.8862+0.0002) g/cm^3 and (1.8137+0.0025) g/cm^3 respectively. The measured bulk density revealed that nickel oxide filled activated palm kernel shell is denser than nickel oxide filled coconut shell.

The FTIR spectra for the raw material samples and activated carbon samples are presented in Figures 1 and 2 respectively. Table 1 summarises the results obtained from FTIR spectroscopy for the raw powder samples designated powder coconut shell (PCS), powder palm kernel shell (PPS) and their mixture (PCS+PPS) and the activated samples designated activated coconut shell (ACS), activated palm kernel shell (APS) and the activated mixture (ACS+APS). The FTIR spectral were interpreted by assigning functional groups to their corresponding absorption bands and these are discernable by their corresponding peak values.

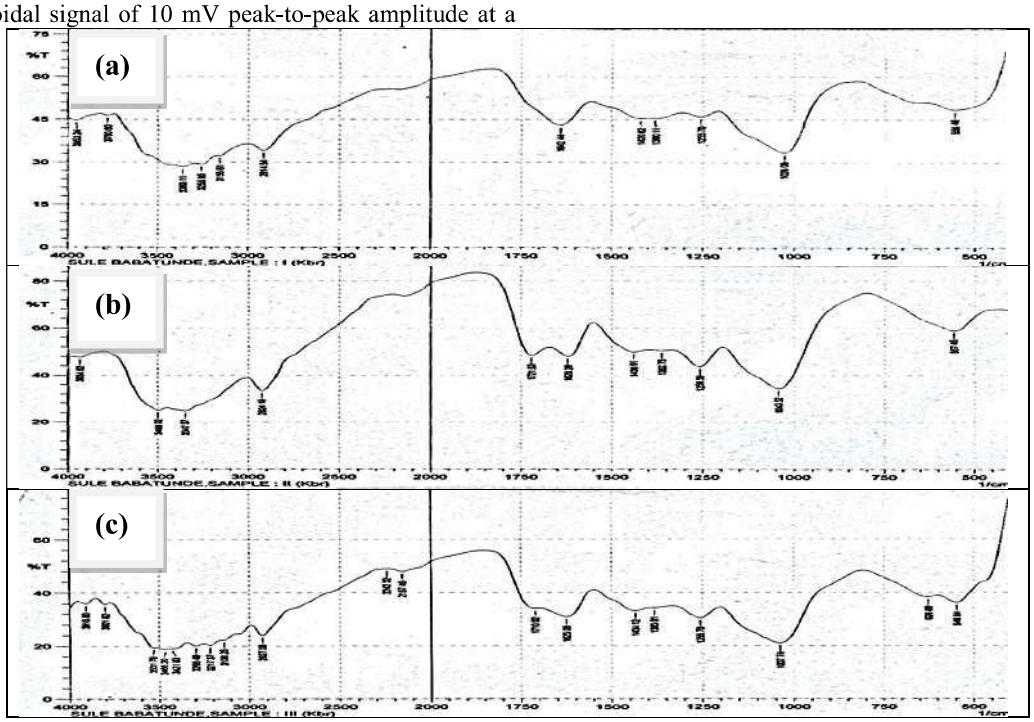

Figure 1: FTIR Spectra of (a) Powdered Coconut shell (PCS) (b) powdered palm kernel shell (PPS) and (c) Powdered mixture of coconut shell and palm kernel shell (PCS+PPS)

It is an established fact that the fundamental vibrations of solids (finger prints) are localized in the low frequency region (<1200 cm^{-1}) of the midrange (400-4000 cm^{-1}) of the infrared (IR) spectrum. It was also reported that the metallic bonds with hydrogen and oxygen are clearly located in the range below 800 cm^{-1} up to about 1900 cm^{-1}(Markova-Deneva 2010). In this work, the significant absorptions observed below 800 cm^{-1} represent metallic bond with oxygen and hydroxyl groups. Furthermore, the small absorptions observed for the organics indicates their presence in minute quantities on the surfaces of the metal oxide filled activated carbon. The prominent functional groups in the samples are basically the hydroxyl groups, alcohols and carbonyl groups comprising of OH stretching vibrations, CH_2 stretching and bending vibrations, CH_3 bending vibrations, C-OH stretching and bending vibrations, CH bending and C=O stretching vibration.

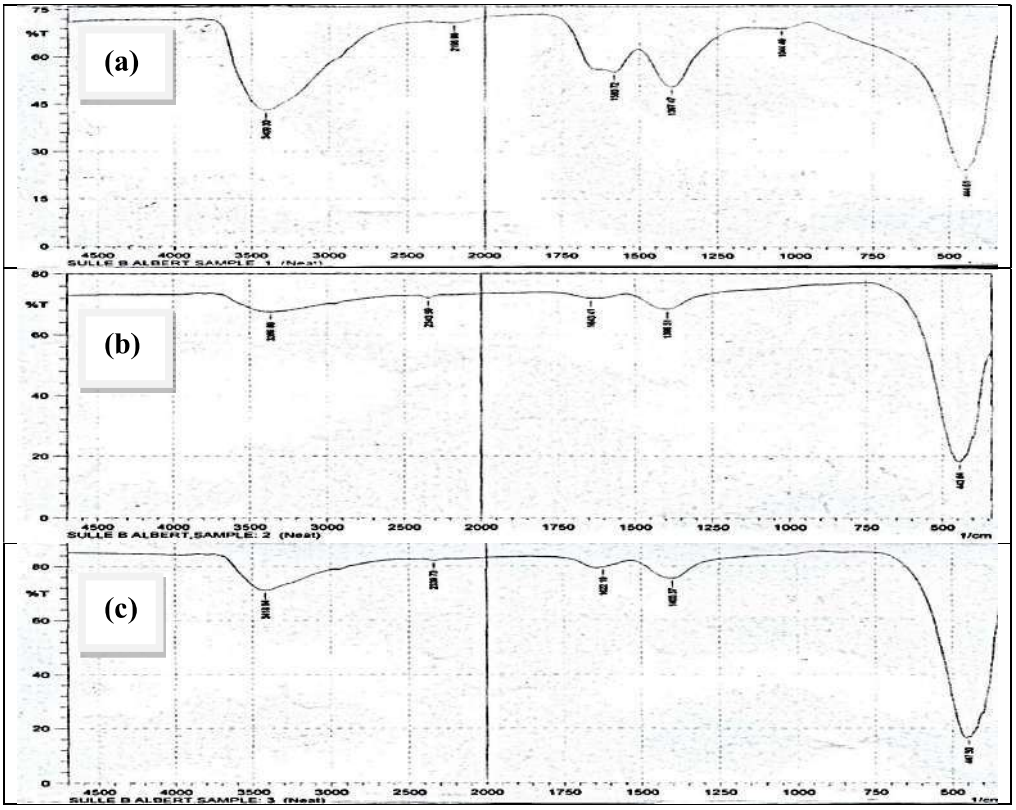

Figure 2: FTIR Spectra of (a) Nickel oxide filled activated coconut shell (ACS), (b) Nickel oxide filled activated palm kernel shell (APS) and (c) Nickel oxide filled activated mixture of coconut shell and palm kernel shell (ACS+APS)

In addition to the broad band representing the stretching vibrations of hydrogen bonded surface water molecules and hydroxyl groups occurring at 3264.63 cm^{-1}-3512.49 cm^{-1}, there exists a band spanning the range 1642.44 cm^{-1} -1580.72 cm^{-1} associated with H_2O bending vibration implying the existence of lattice water. The functional group appearing at 1710.92cm^{-1} -1721.53cm^{-1} represents the carbonyl absorptions. The changes observed in the vibration frequency of vC=O indicates that the addition of NiO has suppressing tendency on the vibration frequency of vC=O because of conjugation with organic groups (vCH_2) as a result of resonance effect leading to an increase in C=O bond length. Finally, the functional group appearing at 443.64cm^{-1} - 447.5cm^{-1} represents Ni-O stretching vibration.

Figure 3(a)-(c) shows SEM micrographs of nickel oxide filled activated coconut shell, nickel oxide filled activated palm kernel shell and nickel oxide filled activated mixture coconut shell and palm kernel shell. The figure depicts high magnification images revealing highly dense and porous structures needed for fast ion transport in high performance supercapacitors. The variation in contrast of the images revealed the NOFAC samples to be a two-phase system interspersed by nickel oxide. The dark phase associated with the host matrix (activated carbon) is overlaid by the light phase associated with the filler (nickel oxide). The resultant particle size analysis was obtained using imaging software (Image-J) and this revealed the average particle size of nickel oxide filled- coconut shell, palm kernel shell and their mixture to be (127.16+44.76) nm, (114.07+45.81) nm and (108.24+44.33) nm respectively

Figure 4 (a) – (c) shows the XRD patterns for nickel oxide filled activated carbon samples. The complex XRD pattern shown in Figure 4 (a) - (c) is a combination of the pattern for graphite (carbon), nickel oxide and nickel hydroxide structures. The XRD patterns shown in Figure 4 (a) and (b) are characterized by more number of peaks indicating reflections typically of an amorphous phase and a two dimensional phase having orientationally disordered layers (Mohammadyani *et al.* 2012) while the XRD pattern shown in Figure 4 (c) is characterized by reduced number of peaks and this can be attributed to the modulating effect of the intensity of the crystalline phases in both components. As such the degree of crystallinity in the mixture component is high. It is noted that all the XRD peaks are identified to graphite and nickel oxide peaks. In all the XRD patterns depicted in Figure 4 (a) - (c), the most prominent peak used to identify graphite structure occurs at $2\theta = 25^o$, but in this patterns the intensity is very low revealing amorphous graphitic carbon phase while others exist at positions described by $2\theta = 45^o$, 55^o and 76^o (JCPDS: 00-008-0415) while the most prominent crystalline phases associated with nickel oxide occur at the following $2\theta = 36^o$, 44^o, 63^o, 79^o (JCPDS: 22-1189) and nickel hydroxide at the following $2\theta = 10^o$, 23o, 34^o, 59^o, (JCPDS: 38-0715).

Table 1: Band assignment of the peaks obtained from the FTIR spectra for the raw material samples and activated carbon samples.

Band Assignment	Absorption Band (cm^{-1})					
	Raw Sample			Activated Sample		
	PCS	PPS	PCS+PPS	ACS	APS	ACS+APS
Intermolecular Hydrogen Bonding (OH stretching vibration)	3264.63	3498.02	3200-3512.49	3409.30	3366.86	3418.94
Free NH stretching vibrations	3156.61-3360.11	3347.57	3139.25	-	-	-
CH_2 (CH stretching vibration)	-	2924.18	2927.08	-	-	-
Non-Conjugated (C≡N stretching vibration)	-	-	2242.32	2196.99	-	-
Non-Conjugated (C=O stretching vibration)	-	1721.53	1710.92	-	-	-
OH (bending vibration)	1642.44	1620.26	1625.08	1580.72	1643.41	1622.19
CH_2 (CH bending vibration)	1420.62	1439.91	1434.12	-	-	-
CH_3 (CH bending vibration)	1380.11	1362.75	1383.01	1397.07	1396.51	-
C-OH stretching vibration	1028.09	1043.52	1039.74	1044.49	-	-
C-OH (OH bending vibration)	556.48	557.0	546.84	-	-	-
Ni-O (stretching vibration)	-	-	-	444.61	443.64	447.5

.

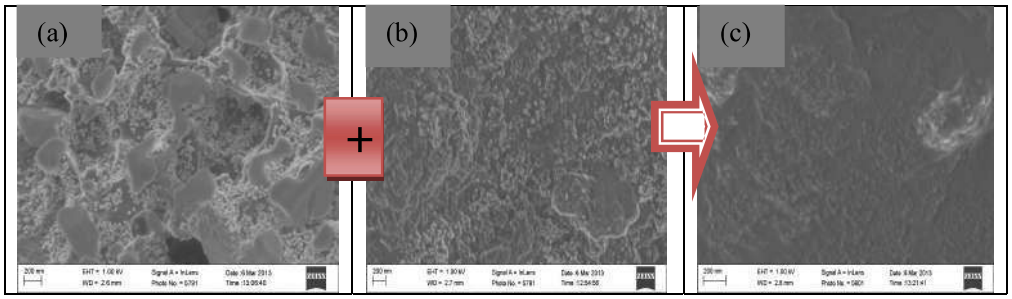

Figure 3: Micrograph of (a) Nickel oxide filled activated coconut shell (b) Nickel oxide filled activated palm kernel shell and (c) Nickel oxide filled activated mixture of coconut shell and palm kernel shell.

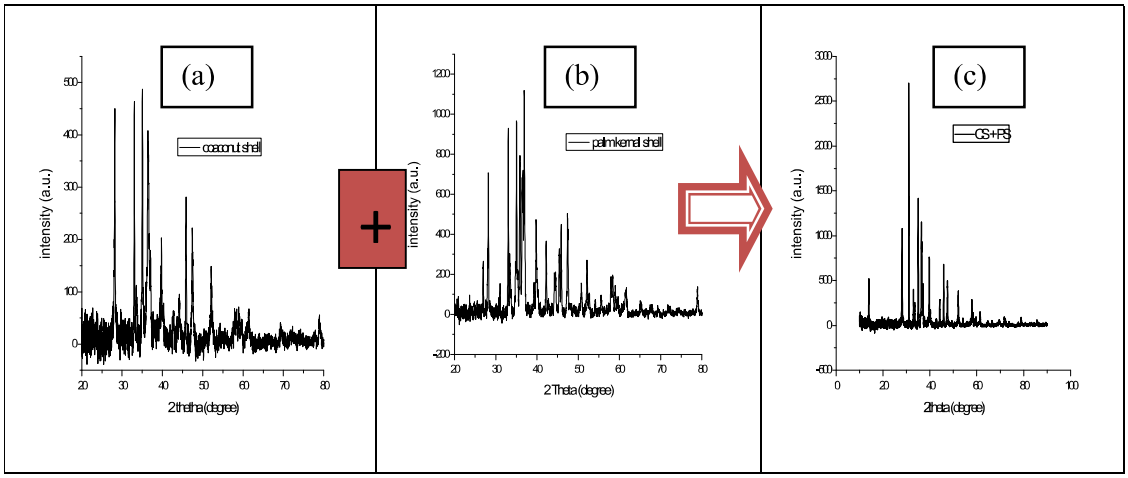

Figure 4: XRD pattern for (a) Nickel oxide filled activated coconut shell (b) Nickel oxide filled activated palm kernel shell and (c) Nickel oxide filled activated mixture of coconut shell and palm kernel shell.

Nyquist plot for the respective supercapacitor cell assemblies based on NOFAC for CS, PS and their mixture in 6M KOH aqueous solution are presented in Figure 5 with an inset showing the expanded high frequency region of the same plot. It can be seen from Figure 5 and the inset, that the cells show a pronounced semicircle at high frequencies implying the charge transfer controlled regime and a straight line at low frequencies indicating the capacitive regime. The impedance plots obtained for these supercapacitor cell assemblies are in line with that of transmission line model (TLM) for the porous electrodes described in the literature (Conway 1999).

Figure 6 (a) – (d) shows the cyclic voltammogram of the supercapacitor cell assemblies based on Nickel Oxide filled Activated Carbon (NOFAC) for Coconut Shell (CS), Palm kernel Shell (PS) and their mixture (CS+PS) in 6M KOH aqueous solution as the electrolyte. The figure depicts a rectangular shaped voltammogram with a large current separation and symmetric in both cathodic and anodic directions obtained for the three cell assemblies. The potential scan was varied from 25 to100 mV/s. A clear capacitive behaviour can be seen from the voltammograms; an established fact arising from the large current separation between the forward and reverse scans with no visible redox peak formation. It can also be seen that the voltammograms are symmetrical about the current zero axis. The fact that all the CVs show rectangular features at the selected scan rates with high current values indicates a good electrochemical activity and high power density.

The galvanostatic charge-discharge analysis of the supercapacitor cell assemblies were performed at four different current densities namely 2.5 mA to 10 mA and from this analysis, the charge storage capacity and durability of the cycle lifetime were obtained. Figure 7 (a) – (c) shows the typical charge-discharge profiles of the respective supercapacitor cell assemblies based on NOFAC for CS, PS and their mixture in 6M KOH aqueous solution. We have used voltage range of 0 to 0.5 V in order to evaluate the performance of these supercapacitors at different voltages. It can be seen that the charge – discharge profiles deviate from the typical linear variation of voltage with time normally exhibited by a purely electrochemical double layer capacitor (EDLC) for lower current values of 2.5 mA and 5.0 mA, which conforms to the proposed model described in the literature (Conway 1999). While the linear behaviour emanating at higher current values of 7.5 mA and 10 mA, is an indication of the formation of a good electrode/electrolyte interface with a well-defined conductivity.

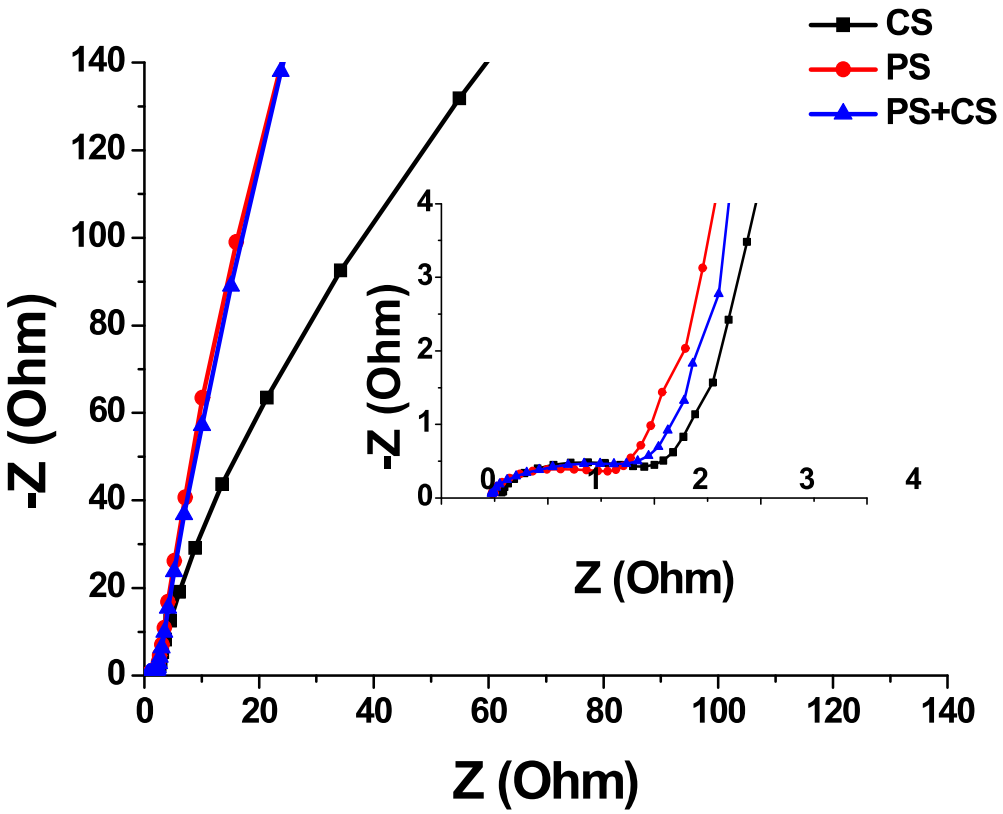

Figure 5: (a) Electrochemical Impedance Spectroscopy for coconut shell (CS), Palm Kernel Shell (PS) and their mixture (CS + PS)

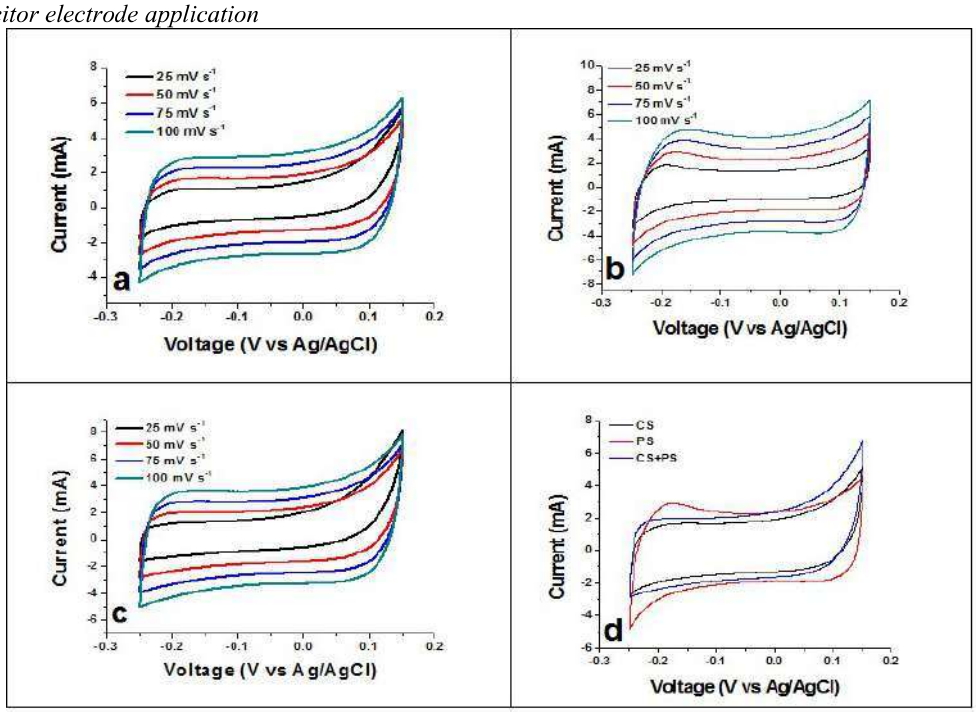

Figure 6: Scan rate studies (a) Cyclic voltammetry curves of Coconut shell (CS) at different scan rates (b) Cyclic voltammetry curves of Palm kernel shell (PS) at different scan rates (c) Cyclic voltammetry curves of mixture of Coconut shell (CS) and Palm kernel shell (PS) at different scan rates and (d) comparison of the three samples at 50 mV s^{-1}.

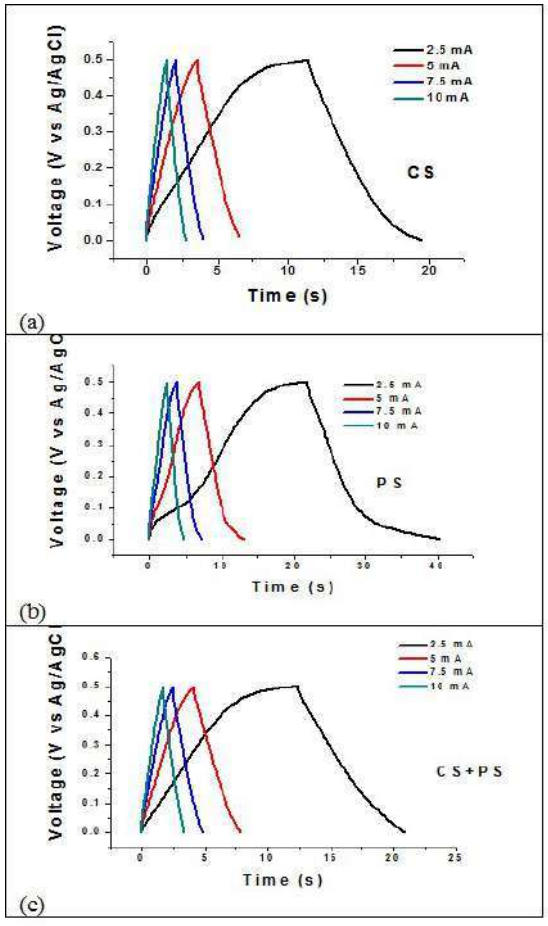

Figure 7: Galvanostatic charge-discharge curve for (a) coconut shell (CS), (b) Palm Kernel Shell (PS) and (c) their mixture (CS + PS).

Figure 8 depicts the specific capacitance for the NOFAC supercapacitor assemblies. A specific capacitance of 44 F/cm^2 was obtained at a constant current of 2.5 mA/cm^2 for the supercapacitor cell assembly based on nickel oxide filled activated coconut shell, a specific capacitance of 95 F/cm^2 was obtained at constant current of 2.5 mA/cm^2 for the supercapacitor assembly based on nickel oxide filled activated palm kernel shell while for the supercapacitor assembly based on nickel oxide filled activated mixture of CS and PS, a specific capacitance of 40 F/cm^2 was obtained at a constant current of 2.5 mA/cm^2. Infact, the specific capacitance decreases to a large extent with the number of cycles for higher current densities to 21 F/cm^2, 32 F/cm^2 and 44 F/cm^2 at 10 mA/cm^2 for supercapacitor assembly based on NOFAC CS, PS and CS+PS respectively. Thus, the supercapacitor cell assembly based on NOFAC palm kernel shell shows better electrochemical properties.

4.0 Conclusions

The microwave-assisted activation technique has been successfully adopted for the production of nickel oxide filled activated carbon for supercapacitor electrode application. The FTIR spectroscopy results confirmed the existence of strong interfacial interaction between NiO and the host matrices showing creation and annihilation of absorption bands in the IR spectra. This interaction revealed the existence of NiO oxide as an inclusion in the NOFACs with significant absorptions observed below 500cm^{-1}. The high magnification SEM images revealed highly dense and porous structures required for fast ion transport in high performance supercapacitors. The XRD analysis confirmed the NOFAC to be a three-phase system with all the XRD

peaks identified to be graphite, nickel oxide and nickel hydroxide structures. The cell assemblies tested in this study attained very good electrochemical performance based on common techniques for testing electrodes such as cyclic voltammetry (CV), Galvanostatic charge/discharge (GCD), and electrochemical impedance spectroscopy (EIS). A rectangular shaped voltammogram with a large current separation and symmetric in both cathodic and anodic directions for the three cell assemblies indicate a clear capacitive behaviour, a good electrochemical activity and high power density. The specific capacitance values of 44 F/cm^2, 95 F/cm^2 and 40 F/cm^2 were obtained at 2.5 mA/cm^2 for the supercapacitor assemblies based nickel oxide filled activated coconut shell, palm kernel shell and their mixture respectively. Thus, nickel oxide filled activated palm kernel shell paraded in this study, with better current response, higher value of specific capacitance and better electrochemical behaviour can be used for production of supercapacitor electrodes.

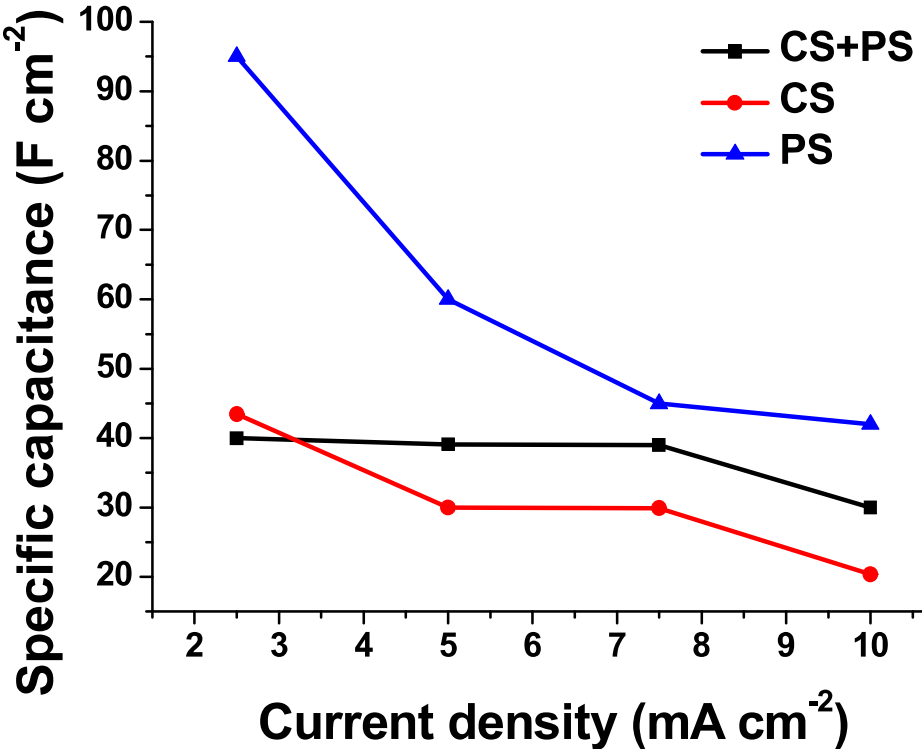

Figure 8: Specific capacitance for coconut shell (CS), Palm Kernel Shell (PS) and their mixture (CS + PS).

Acknowledgement

Authors would like to acknowledge the technical assistance rendered by A. BELLO of the Department of Physics, Institute of Applied Materials under the SARCHI Chair in Carbon Technology and Materials, University of Pretoria, Pretoria 0028, South Africa.

References

Acevedo, B., Barriocanal, C., Lupul, I. and Gryglewicz, G. (2015). Properties and performance of mesoporous activated carbons from scrap tyres, bituminous waste and coal. Fuel, 151: 83-90.

Aravanda, L.S., Bhat, U. and Ramachandra, B. (2013). Binder free MoO3/multi-walled carbon nanotube thin film electrode for high energy density supercapacitor. Electrochim. Acta. 112: 663-669.

Baghbanzadeh, M., Carbone, L., Cozzoli, P.D. and Kappe, C.O. (2011). Microwave-assisted synthesis of colloidal inorganic nanocrystals. Angew, Chemie Int. Ed., 50: 1127-1139.

Bello, A., Barzegar, F., Momodu, D., Taghizadeh, F., Fabiane, M. and Dangbegnon, J. (2014). Morphological characterization and impedance spectroscopy study of porous 3D carbons based on graphene foam-PVA/Phenol-formadehyde resin composite as an electrode material for supercapacitors. RSC. Adv., 4: 39066-39072.

Conway, C.E. (1999). Electrochemical Supercapacitors: Scientific, Fundamental and Technologcial Applications. Kluwer Academic/Plenum, New York.

Demarconnay, L., Raymundo-Pinero, E. and Begiun, F. (2011). Adjustment of electrodes potential window in an asymmetric Carbon/MnO_2 supercapacitor. J. Power Sources, 196: 580-586.

Ge, X., Tian, F., Wu, Z., Yan, Y., Cravotto, G. and Wu, Z. (2015). Adsorption of naphthalene from aqeous solution on coal-based active modified by microwave induction: Microwave power effect. Chem. Eng. Process. Process Intensif, 91:67-77.

Halper, M.S. and Ellenbogen, J.C. (2006). Supercapacitors: A brief Overview. MITRE Nanosystems Group: Project no: 15055224,

The MITRE Corporation; McLean Virginia, USA.

Jampani, P., Manivannan, A. and Kumta, P.N. (2010). Advancing the supercapacitor materials and technology frontier for improving Power Quality. The Electrochemical Society Interface, Fall 2010.

Kappe, C.O (2008).Microwave dielectric heating in synthetic organic chemistry. Chem. Soc. Rev., 37: 1127-1139.

Markova-Deneva, I. (2010). "Infrared spectroscopy investigation of metallic nanoparticles based on copper, cobalt and nickel synthesized through borohydride reduction method". Journal of the University of Chemical Technology and Metallurgy, 45(4): 351-378.

Mohammadyani, D., Hosseini, S.A. and Sadrnezhaad, S.K. (2012). Characterization of nickel oxide nanoparticles synthesisized via rapid microwave-assisted route. International Journal of Modern Physics: Conference Series, 5: 270-276.

Momcilovic, M., Purenovic, M., Bojic, A., Zarabica, A. and Randelovic, M. (2011). Removal of lead (II) ions from aqueous solutions by adsorption onto pine cone activated carbon. Desalination, 276: 53-59.

Nunell, G.V., Ferdinandez, M.E., Borelli, P.R. and Cukierman, A.L. (2015). Nitrate uptake improvement by modified activated carbons developed from two species of pine cone. J. Colloid Interface Sci., 440: 102-108.

Ofomaja, A.E. and Naidoo, E. B. (2011). Bisorption of copper from aqueous solution by chemically activated pine cone: A kinetic study. Chem. Eng. J. 175: 260-270.

Park, S., Liang, C., Sheng, D., Dudney, N. and DePaoli, D. (2006). Mesoporous carbon Materials as electrode for electrochemical double layer capacitor. MRS Proc. 973: 903-916.

Roberts, M.E., Wheeler, D.R, McKenzie, B.B. and Bunker, B.C. (2009). High specific capacitance conducting polymer supercapacitor electrodes based on poly [tris(thiophenylphenyl)amine]. J. Mater. Chem., 19: 6977-6979.

Salame, I.I. and Bandosz, T.J. (2001). Surface chemistry of activated carbons: Combining the results of temperature-programmed desorption, boehm and potentiometric titrations. J. Colloid Interface Sci., 240: 252-258.

Taberna, P.L., Simon, P. and Fauvarque, J.-F. F. (2003). Electrochemical characteristics and impedance spectroscopy studies of carbon-Carbon supercapacitors. J. Electrochem. Soc., 150: A292-A300.

Tang, W., Liu, L., Tian, S., Li, L., Yue, Y., Wu, Y. and Zhu, K. (2011). Aqeuos Supercapacitor of High Energy Density based on MoO_3 Nanoplates as anode Material. Chem. Commun. 47: 10058-10060.

Wang, H, Casalongue, H.S., Liang, Y. and Dai, H. (2010). $Ni(OH)_2$ nanoplates grown on graphene as advanced electrochemical pseudocapacitor materials. J. Am Chem. Soc. 132: 7472.

Wu, M. –S. and Hsieh, H. –H. (2008). Nickel Oxide/Hydroxide Nanoplate synthesized by chemical precipitation for electrochemical capacitors. Electrochim. Acta., 53: 3427-3435.

Yang, H., Peng, J., Srinivasakannan, C., Zhang, L., Xia, H. and Duan, X. (2010). Preparation of high surface area activated carbon from coconut shells using microwave heating. Biorsour. Technol., 6163-6169.

Zhang, W., Ma, C., Fang, J., Cheng, J., Zhang, X. and Dong, S. (2013). Asymmetric electrochemical capacitors with high energy and power density based on graphene/CoAl-LDH and activated carbon electrodes. RSC. Adv., 3: 2483-2490.